Employment of curvilinear coordinates in *ab initio* calculations of insulators using pseudopotentials

A. S. Fedorov

L. V. Kirenskiĭ Institute of Physics, Russian Academy of Sciences, Siberian Branch, 660036 Krasnoyarsk, Russia

The standard *ab initio* scheme for calculating the structure of crystals using nonlocal pseudopotentials is modified for use in curvilinear coordinates. A method for solving the Poisson equation for the Coulomb potential in a curved space in the *k* representation is found. It is shown in the example of calculations for crystals of insulators having an NaCl structure that the employment of a curved space permits a very significant decrease in the required size of the basis set. © *1999 American Institute of Physics.* [S1063-7834(99)01102-8]

In the last decade, technological developments and a heightened interest in the description of complex microscopic and macroscopic structures have led to a need for *ab initio* calculations of complex structures with tens, hundreds, and thousands of atoms in the unit cell. The inclusion of dynamics in such calculations[1–4] using molecular dynamics, which was proposed in Ref. 5, as well as determination of the response of systems to various disturbances (calculations of phonon spectra etc.), call for the availability of simple *ab initio* calculation schemes, which can easily be modified for application to the tasks required. Unfortunately, the existing methods either were too complicated for modification (the methods based on solving the Schrödinger equation for MT spheres, viz., the LMTO method and the full-potential method) or required large amounts of machine resources (in particular, the pseudopotential method for describing atoms with large pseudopotentials required the use of a basis set consisting of more than 1000 plane waves even for simple structures consisting of several atoms).

Some new effective calculation methods have appeared in the last 5–7 years. The use of ultrasoft pseudopotentials, which was proposed in Ref. 6, significantly reduced the deficiencies of the classical pseudopotential method at the expense of only slight complication of the calculation scheme.

Another new promising method, which was proposed in Ref. 7, is a hybrid of the LMTO method and the pseudopotential method and permits avoiding many deficiencies of both methods.

At the same time, a new approach to the solution of the Kohn–Sham equations within a pseudopotential scheme was proposed within Car–Parinello molecular dynamics in Refs. 1 and 2 (as well as Refs. 3 and 4). This approach was based on replacement of the basis functions in the form of the ordinary plane waves $|k\rangle \equiv (1/\sqrt{\Omega})\, e^{i\mathbf{k}\cdot\mathbf{r}}$ by curved plane waves of the form $|k\rangle \equiv (1/\sqrt{\Omega})\, |\partial\boldsymbol{\xi}(\mathbf{r})/\partial\mathbf{r}|^{1/2} e^{i\mathbf{k}\cdot\boldsymbol{\xi}(\mathbf{r})}$. It is easy to show that such waves form an orthonormalized basis set and that the matrix elements of the Hamiltonian in this basis set transform into matrix elements that can be calculated in a basis set of ordinary plane waves, but in a special

curved space that can be described by the mutually one-to-one mapping $\boldsymbol{\xi} = \boldsymbol{\xi}(\mathbf{r})$.

This paper proposes a modification of the approach just cited, which does not employ molecular dynamics, since for a small number of basis functions the latter formalism does not have any advantages over the classical direct method for diagonalization of the Hamiltonian.

I. CALCULATION SCHEME

The standard calculation scheme for the pseudopotential method described in Ref. 8 was used in the calculation algorithm. Norm-conserving pseudopotentials, which were calculated and tabulated in Ref. 9, served as the pseudopotentials. The exchange-correlation effects were taken into account within the density functional formalism [the local-density approximation (LDA)] using the approximation from Refs. 10 and 11.

All the physical quantities (wave functions, local and nonlocal parts of the potentials, Hamiltonians, and electron density) were calculated using basis functions of the form $\chi_k(\mathbf{r}) \equiv |k\rangle = (1/\sqrt{\Omega})\, |\partial\boldsymbol{\xi}(\mathbf{r})/\partial\mathbf{r}|^{1/2} e^{i\mathbf{k}\cdot\boldsymbol{\xi}(\mathbf{r})}$, which, like ordinary plane waves, are orthonormalized:[1]

$$(k|k') = \frac{1}{\Omega} \int\int\int_\Omega d^3r \left(\left| \frac{\partial\boldsymbol{\xi}(\mathbf{r})}{\partial\mathbf{r}} \right| e^{i(\mathbf{k}'-\mathbf{k})\boldsymbol{\xi}(\mathbf{r})} \right)$$

$$= \frac{1}{\Omega} \int\int\int_\Omega d^3\xi \, (e^{i(\mathbf{k}'-\mathbf{k})\boldsymbol{\xi}}) = \delta_{\mathbf{k},\mathbf{k}'}.$$

Here $|\partial\boldsymbol{\xi}(\mathbf{r})/\partial\mathbf{r}| = g_{ij}^{-1/2}$, where the metric tensor $g_{ij} = (\partial r^k/\partial\xi^i)\,\partial r^k/\partial\xi^j$.

Going over from the space $\mathbf{r}$ to the space $\boldsymbol{\xi}$ in the calculation of the matrix elements of the Hamiltonian, as well as the potentials and the electron density, in the basis set under consideration, we can easily see that the expressions for them become the same as in the case of plane waves, but in the space $\boldsymbol{\xi}$, with the exception of the forms of the Laplacian in the kinetic energy operator.

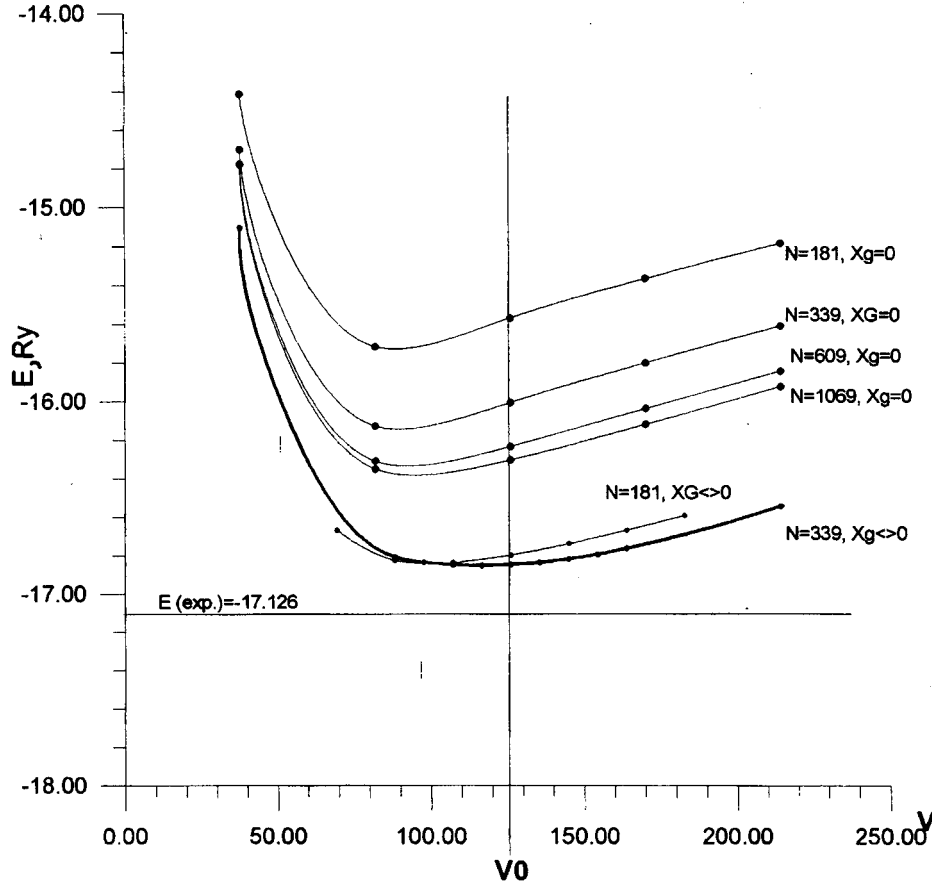The Kohn–Sham equations in reciprocal space have the form

FIG. 1. Dependence of the binding energy E on the unit-cell volume V and on the number of plane waves and curved plane waves for MgO.

$$H^\nu(g,g')\chi^\nu(g') = \varepsilon^\nu \chi^\nu(g),$$

where χ^ν is an eigenvector (wave function), which can be expanded for each ν in the basis set $\chi^n_{k+g}(\mathbf{r})$ according to the formula

$$\chi^\nu(\boldsymbol{\xi}(\mathbf{r})) = \frac{1}{\sqrt{\Omega}} \sum_g \chi^\nu_k(g) \left| \frac{\partial \boldsymbol{\xi}(\mathbf{r})}{\partial \mathbf{r}} \right|^{\frac{1}{2}} e^{i(\mathbf{k}+\mathbf{g})\boldsymbol{\xi}(\mathbf{r})}, \qquad (1)$$

and ε^ν is an eigenvalue of the Schrödinger equation with the wave function $\mathbf{k}$ and the spin σ in zone n. In (1) $\nu = \{\mathbf{k}, \sigma, n\}$, $\mathbf{k}$ is the wave vector in the first Brillouin zone, $\mathbf{g}$ is the reciprocal lattice vector, and n is the number of the zone.

The matrix elements of the Hamiltonian $H = -(\hbar^2/2m)\, d^2/dr^2 + \hat{V}$ in this basis set have the following form:

$$\langle q|H|q'\rangle = \langle q|T + V_{nl}|q'\rangle$$

$$+ \frac{1}{\Omega} \int \int \int_\Omega d^3\xi \, (V_l(\boldsymbol{\xi}(\mathbf{r})) e^{i(\mathbf{q}'-\mathbf{q})\boldsymbol{\xi}}),$$

$$\langle q|T|q'\rangle = \frac{1}{\Omega} \int \int \int_\Omega d^3\xi \left(\left(\frac{\hbar^2}{2m} [(\mathbf{q}_i - iA_i) \right. \right.$$

$$\left. \left. \times g^{ij}(\mathbf{q}'_j + iA_j)] \right) e^{i(\mathbf{q}'-\mathbf{q})\xi} \right), \qquad (2)$$

where $\langle q|T|q'\rangle$ describes the Laplacian in the basis set $(1/\sqrt{\Omega})\, |\,\partial\boldsymbol{\xi}(\mathbf{r})/\partial\mathbf{r}\,|^{1/2e^{i\mathbf{k}\cdot\boldsymbol{\xi}(\mathbf{r})}}$ (see Ref. 1) and where g^{ij} denotes the tensor which is the inverse of the metric tensor g_{ij}, and the scale potential $A_i = (1/2)\partial/\partial\xi' \log|\partial r/\partial\xi|$ appears upon differentiation of the basis function. The total potential can be divided into a nonlocal part $\langle q|V_{nl}|q'\rangle$ and a local potential $V_l(q-q') \equiv \int_\Omega d^3 r\, (V_l(\boldsymbol{\xi}(\mathbf{r})) e^{i(\mathbf{q}'-\mathbf{q})\boldsymbol{\xi}(\mathbf{r})})$. The local potential can be divided, in turn, into the Coulomb potential, the exchange-correlation potential, and the local part of the pseudopotential:

$$V_l(\boldsymbol{\xi}(\mathbf{r})) \equiv V_{\mathrm{Coul}}(\boldsymbol{\xi}(\mathbf{r})) + V_{\mathrm{xc}}(\rho(\boldsymbol{\xi}(\mathbf{r}))) + V_l^{\mathrm{ps}}(\boldsymbol{\xi}(\mathbf{r})).$$

The matrix elements of the exchange-correlation potential and the local part of the pseudopotential $(k|V(\boldsymbol{\xi}(\mathbf{r}))|k')$ were calculated by Fourier transformation from the values on the uniform grid $\boldsymbol{\xi}(\mathbf{r})$.

The exchange-correlation potential V_{xc} in the local-density approximation and the exchange-correlation energy $\Phi_{\mathrm{xc}} = \int_\Omega d^3 r\, (\varepsilon_{\mathrm{xc}}(\rho)\rho(\boldsymbol{\xi}(\mathbf{r})))$, where $\varepsilon_{\mathrm{xc}}(\rho)$, i.e., the exchange-correlation energy density, were taken from Ref. 10:

$$V_{\mathrm{xc}}(\boldsymbol{\xi}(\mathbf{r})) = \frac{\partial \Phi_{\mathrm{xc}}}{\partial\rho(\mathbf{r})}, \qquad (3)$$

$$V_{\mathrm{xc}}(g) = \frac{1}{\Omega} \int \int \int_\Omega d^3 r\, (V_{\mathrm{xc}}(\boldsymbol{\xi}(\mathbf{r})) e^{-i\mathbf{g}\boldsymbol{\xi}(\mathbf{r})}), \qquad (4)$$
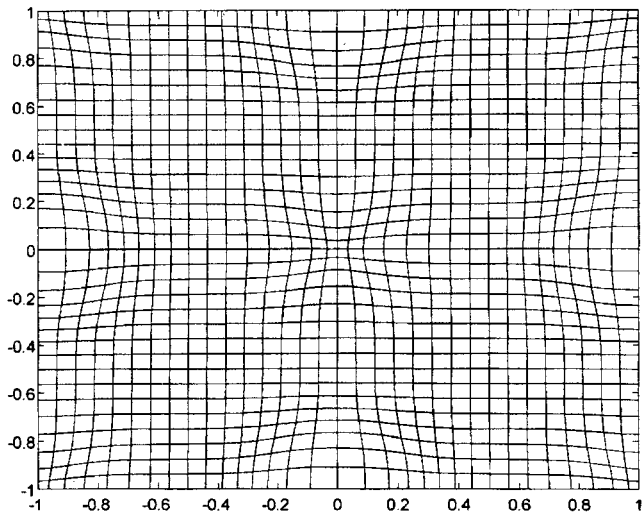
FIG. 2. Best mapping $\xi = \xi(\mathbf{r})$ ($N = 339$) for MgO.

$$V_l^{ps}(g) = \frac{1}{\Omega} \int \int \int_{\Omega} d^3 r \, (V_l^{ps}(\xi(\mathbf{r})) e^{-i\mathbf{g}\xi(\mathbf{r})}). \qquad (5)$$

The matrix elements of the nonlocal part of the pseudopotential have the form

$$(k|V_{nl}|k') = \sum_{i,l,m} (k(\xi(\mathbf{r}))|Y_{lm}(\mathbf{r})\rangle V_{lm}(r)$$

$$\times \langle Y_{lm}(\mathbf{r})|k'(\xi(\mathbf{r}))) e^{-i\mathbf{R}_i^0(\mathbf{k}-\mathbf{k}')}. \qquad (6)$$

The electron density is expressed in the following manner

$$\rho(\xi(\mathbf{r})) = \sum_{\nu} \Theta^{\nu} \lambda^{\nu*}(\xi(\mathbf{r})) \chi^{\nu}(\xi(\mathbf{r})), \qquad (7)$$

$$\rho(g) = \sum_{\nu, g'} \Theta^{\nu} \chi_{k+g'}^{\nu*} \chi_{k+g+g'}^{\nu}. \qquad (8)$$

Here and below Θ^{ν} is the occupation function of level ν.

The calculation of the Coulomb potential in the basis set $(1/\sqrt{\Omega}) |\partial\xi(\mathbf{r})/\partial\mathbf{r}|^{1/2} e^{i\mathbf{k}\cdot\xi(\mathbf{r})}$ is a nontrivial problem, since while in "flat" space the Laplacian in the k representation has the form of a diagonal matrix $(\mathbf{k}+\mathbf{g})^2 \delta_{g,g'}$, in the curved space $\xi(\mathbf{r})$ the Laplacian has off-diagonal components [see the right-hand side of (2)]. The system of Poisson equations is written in the form

$$\sum_{k''} (k|\Delta|k'')(k''|V_{\text{Coul}}|k') = -4\pi(k|\rho(\xi(\mathbf{r}))|k')$$

$$\equiv -4\pi\rho(\mathbf{k}-\mathbf{k}'). \qquad (9)$$

The matrix of the Laplacian in any complete basis set has a minimum eigenvalue ε^0 equal to 0, which corresponds to the
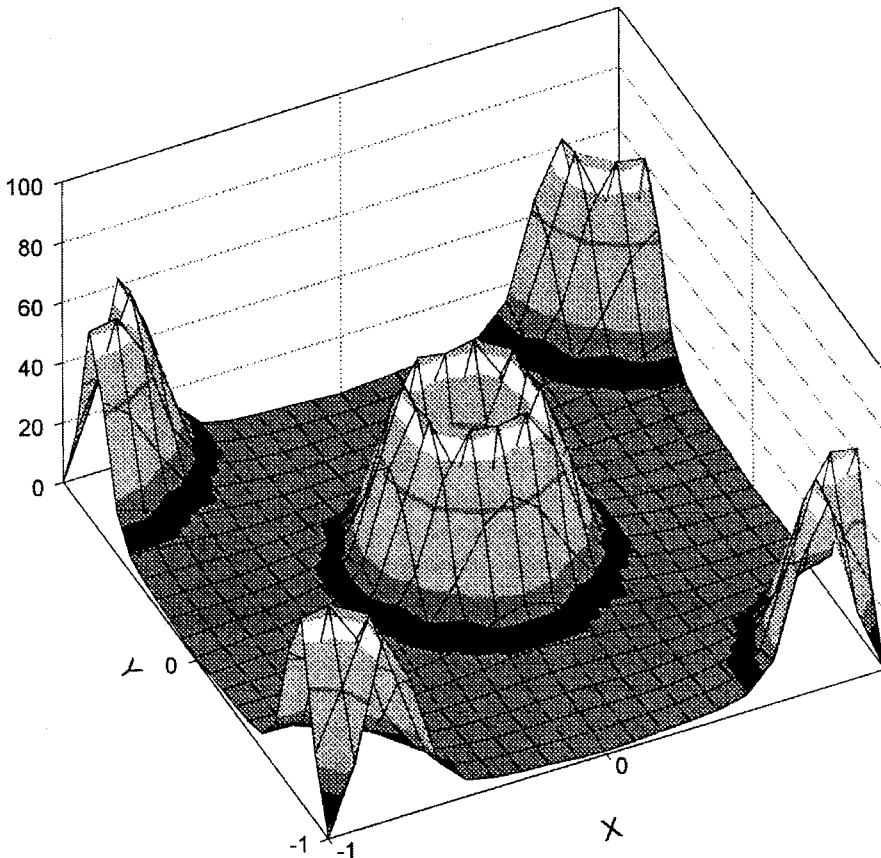

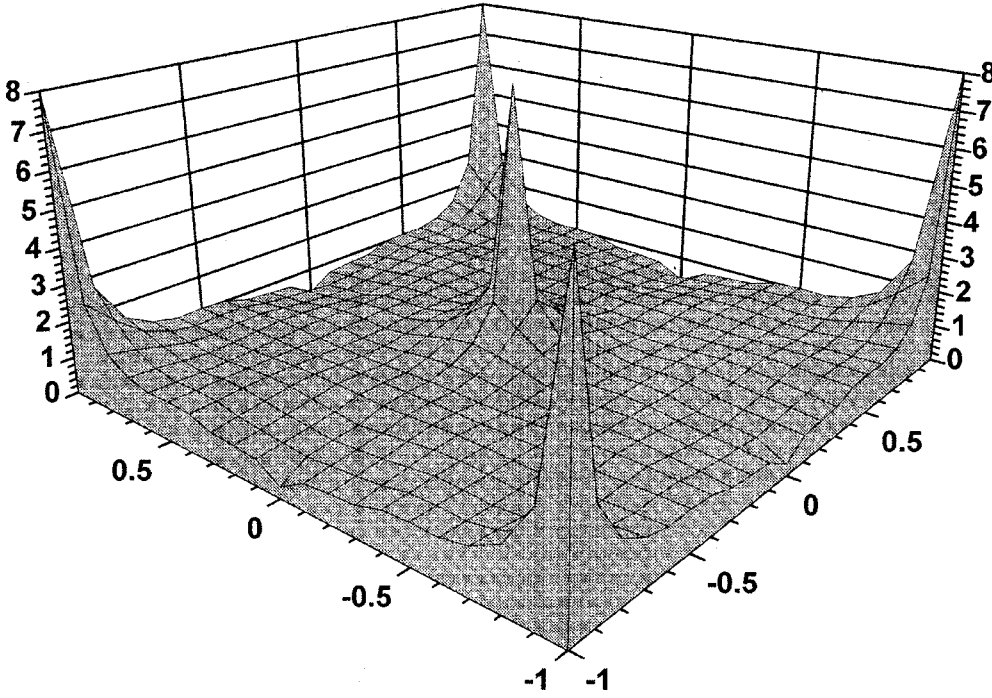FIG. 3. Distribution of the electron density for MgO in $\xi(\mathbf{r})$.

FIG. 4. Distribution of $|\partial\xi(\mathbf{r})/\partial\mathbf{r}|$ for MgO in $\xi(\mathbf{r})$.

solution-constant $C(\xi(\mathbf{r})) = \text{const}$ from the degenerate subspace of eigenvectors in the space $\mathbf{r}$. Choosing $\mathbf{k}' \equiv \widetilde{\mathbf{k}}' + \mathbf{g} = 0$ allows the lowest eigenvector of the Laplacian ε^0 to describe the vector C. However, while the exclusion of this eigenvalue is trivial for a diagonal matrix, this is not the case for an off-diagonal matrix. To solve the system of equations, we utilize the orthogonality of the solution sought $V_{\text{Coul}}(\xi(\mathbf{r}))$ and a vector from the degenerate subspace

$$C(\xi(\mathbf{r})) = \sum_g C(g) \left|\frac{\partial\xi(\mathbf{r})}{\partial\mathbf{r}}\right| e^{i\mathbf{g}\xi(\mathbf{r})}.$$

This is a consequence of the electroneutrality of the crystal

$$\int\int\int_\Omega d^3r \left(V_{\text{Coul}}(\xi(\mathbf{r})) + V_{\text{pseudo}}(\xi(\mathbf{r}))\right) = 0$$

and the choice of the normalization

$$\int\int\int_\Omega d^3r \left(V_{\text{Coul}}(\xi(\mathbf{r}))\right) = 0, \tag{10}$$

whence follows the orthogonality of V_{Coul} and the constant C. Next, choosing $\mathbf{k}' = 0$ in (9) to obtain the minimum eigenvalue of the Laplacian and orthogonalizing the vector of the right-hand side relative to $C(g)(\rho \perp C)$, we can use the algorithms for solving a degenerate system of equations with a right-hand side that is orthogonal to a degenerate eigenvector (which has a unique solution) and go over from solving the system (9) to solving the system (11):

$$\sum_{k''} (k|(\Delta - \varepsilon^0)|k'')(k''|V_{\text{Coul}}|k' = 0)$$

$$= -4\pi(k|\rho(\xi(\mathbf{r}))|k' = 0) \equiv -4\pi\rho(\mathbf{k-0}). \tag{11}$$

In these calculations, because of the incompleteness of the basis set, we have $\varepsilon^0 \approx 3 \times 10^{-4}$, which can serve as an indirect quality factor of the basis set associated with the mapping $\xi(\mathbf{r})$.

Although the relation (10) is satisfied, the curved space imposes the following conditions:

$$V_{\text{Coul}}(g = 0) \neq 0, \quad V_{\text{loc}}(g = 0) \neq 0.$$

The total binding energy of a crystal has the form

$$E/N = E_{\text{Mad}}/N + \frac{bZ}{\Omega} - \frac{1}{2}\sum_g V_{\text{Coul}}(\mathbf{g})\rho(\mathbf{g}) + V_{\text{Coul}}(\mathbf{g} = 0)$$

$$+ V_{\text{ps}}(\mathbf{g} = 0) + \int\int\int_\Omega d^3r \left((\varepsilon_{\text{xc}}(\rho)\right.$$

$$\left. - \mu_{\text{xc}}(\rho))\rho(\mathbf{r})\right) + \frac{1}{N}\sum_\nu \Theta^\nu\varepsilon^\nu, \tag{12}$$

where E_{Mad} is the Madelung electrostatic energy, Z is the total charge of the unit cell, ε_F is the Fermi energy, which can be determined from the condition $Z = 1/N\sum_{\varepsilon^\nu < \varepsilon_F}\Theta^\nu$, and bZ/Ω is the non-Coulomb part of the pseudopotential[12] in the limit $\mathbf{q}\to 0$:

$$\frac{bZ}{\Omega} = \lim_{\mathbf{q}\to 0}\left(\sum_s V_e^s(\mathbf{q}) + \frac{4\pi Ze^2}{\mathbf{q}^2}\right). \tag{13}$$

TABLE I. Equilibrium parameters.

	Unit-cell parameter, Å			Bulk modulus, Mbar		
Crystal	Cartesian	curvilinear	exp.	Cartesian	curvilinear	exp.
MgO	3.74	4.18	4.21 Ref. 13	1.61	1.32	1.53 Ref. 15
BaO	4.03	5.19	5.54 Ref. 14	8.46	0.45	0.74 Ref. 16
NaCl	5.00	5.49	5.63 Ref. 15	0.530	0.238	0.245 Ref. 15
PbS	5.76	5.77	5.92 Ref. 16	0.96	0.763	0.62 Ref. 16

We note that the fictitious term associated with the space deformation energy[1–4] was not used in the Hamiltonian.

The mapping $\xi(\mathbf{r})$ was chosen on the basis of the assumption of a correlation between $|\partial\xi(\mathbf{r})/\partial\mathbf{r}|$ and the electron density and with the goal of describing $\xi(\mathbf{r})$ by a small number of parameters.

On the basis of these considerations the mapping was chosen in the form of the additive sum of the contribution of each atom in the lattice, where each contribution is described by a Gaussian function of two parameters, viz., α and β:

$$\mathbf{r}=\xi-\sum_i\ (\xi-\xi_i^0)\alpha_i e^{-\beta_i(\xi-\xi_i^0)^2}.$$

Here β_i characterizes the space-curving radius of action of the respective ion with the coordinate ξ_i^0, and α_i describes the amplitude of the perturbation of space caused by that ion.

The total energy $E=E(\alpha_i,\beta_i)$ was minimized by direct minimization using a quasi-Newtonian minimization method.

II. RESULTS

The results obtained are presented in Figs. 1–4 and in Tables I and II.

Figure 1 shows the dependence of the binding energy E of a MgO crystal on the unit-cell volume V and on the number of basis functions for both the case of plane waves ($X_g \equiv \{\alpha_i,\beta_i\}\equiv 0$) and the case of curved plane waves ($X_g \neq 0$). It can be seen that the introduction of a curved space for any basis set is equivalent to a very significant increase in the number of basis functions in ''flat'' space. The very slow convergence of the binding energy with increasing size of the basis set in the standard approach can also be seen. The figure also shows the experimental value of the equilibrium unit-cell volume $V0$ and the binding energy from Ref. 17.

Figure 2 shows the best mapping $\xi=\xi(\mathbf{r})$ (for $N=339$) for a MgO crystal in the (001) plane. The figure exhibits thickening of the coordinate grid (along with an increase in the amplitude multiplier $|\partial\xi(\mathbf{r})/\partial\mathbf{r}|^{1/2}$ of the basis functions) in the vicinity of the O ions, where the electron density reaches a maximum, and thinning of the coordinate grid in the vicinity of Mg ions. The curvature parameters for the crystals investigated are listed in Table II.

Figure 3 shows the distribution of the electron density (the coordinate Z) in the (001) plane (the coordinates X,Y) for MgO in the space $\xi(\mathbf{r})$ within the range of nearest neighbors.

Figure 4 shows the distribution of the transition Jacobian $|\partial\xi(\mathbf{r})/\partial\mathbf{r}|$ (the coordinate Z) in the analogous coordinates

X,Y in the same space. A correlation can be seen between the electron density and the Jacobian. This correlation causes significant smoothing of the electron density in the space $\xi(\mathbf{r})$, which leads to a decrease in the effective size of the Hamiltonian in $\xi(\mathbf{r})$ and permits a sharp decrease in the necessary size of the basis set in this space.

Table I lists the equilibrium unit-cell parameters and the values of the bulk modulus in the crystals investigated when flat and curved spaces are used, as well as the experimental values. This table reveals significant underestimation of the unit-cell parameter and an error in the bulk modulus under the ordinary approach for all the crystals studied and considerably better agreement with experiment when curved coordinates are used.

Table II lists the curvature parameters α_i and β_i and the corresponding size of the basis set for all the crystals investigated. It can be seen that in these crystals the anions are described by positive values of α_i (which corresponds to ''thickening'' of the space at sites of larger electron density), while the cations are described by negative values (which correspond to thinning).

Thus, this method seems promising within the pseudopotential approach, since it permits significant (by 10- or more-fold) reduction in the size of the basis set. In addition, the calculation algorithm in ξ space differs only slightly from the standard algorithm. The data obtained reveal significant lowering of the energy in the calculations with a curved basis set, which is a consequence of the inaccurate description of pseudowave functions by plane waves near atoms, where the pseudopotential is most significant and where ''crushing'' of the grid cells owing to the curving of space permits a more exact description of the behavior of the pseudowave functions. Significantly better agreement with experiment can also be seen in the determination of the equilibrium unit-cell parameters.

Additional research aimed at more rapid determination of the optimal characteristics of the curved space would be desirable.

TABLE II. Curvature parameters.

Crystal	α_i	β_i	Basis set size
MgO	0.500/−0.503	0.991/0.688	339
BaO	0.476/−0.191	0.332/0.937	609
NaCl	0.172/−0.352	0.110/0.177	609
PbS	0.101/−0.220	0.992/0.497	339

[1] F. Gygi, Europhys. Lett. **19**, 617 (1992).
[2] F. Gygi, Phys. Rev. B **48**, 11 692 (1993).
[3] D. R. Hamann, Phys. Rev. B **51**, 7337 (1995).
[4] D. R. Hamann, Phys. Rev. B **51**, 9508 (1995).
[5] R. Car and M. Parinello, Phys. Rev. Lett. **55**, 2471 (1985).
[6] D. Vanderbilt, Phys. Rev. B **41**, 7892 (1990).
[7] P. E. Blöchl, Phys. Rev. B **50**, 17 953 (1994).
[8] J. Ihm, A. Zunger, and M. L. Cohen, J. Phys. C **12**, 4409 (1979).
[9] G. B. Bachelet, D. R. Hamann, and M. Schlüter, Phys. Rev. B **26**, 4299 (1982).
[10] J. Perdew and A. Zunger, Phys. Rev. B **23**, 5048 (1981).
[11] D. M. Ceperley and V. J. Alder, Phys. Rev. B **18**, 3126 (1978).
[12] E. G. Brovman and Yu. M. Kagan, Usp. Fiz. Nauk **112**, 369 (1974) [Sov. Phys. Usp. **17**, 125 (1974)].
[13] G. Kalpana, B. Palanivel, and M. Rajagopalan, Phys. Rev. B **52**, 4 (1995).
[14] S. A. Chang, C. W. Tompson, E. Gurnen, and L. D. Muhlestein, J. Phys. Chem. Solids **36**, 769 (1975).
[15] C. Kittel, *Introduction to Solid State Physics*, 5th ed. (Wiley, New York, 1976; Nauka, Moscow, 1978).
[16] *Physical Constants* [in Russian], Énergoatomizdat, Moscow (1991).
[17] M. J. Mehl, R. J. Hemley, and L. L. Boyer, Phys. Rev. B **33**, 8685 (1986).

Translated by P. Shelnitz